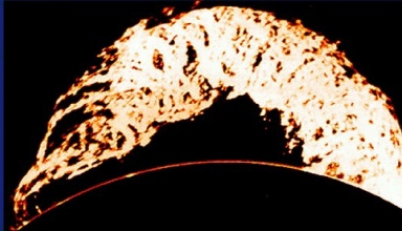
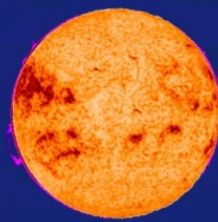
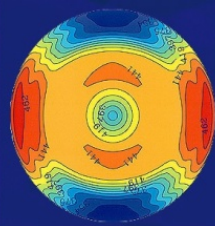


HAO



Perspectives on Ionospheric Electrodynamics



**Arthur D. Richmond, NCAR-HAO
and collaborators**

- Ionospheric dynamo modeling
- Disturbance dynamo
- Assimilative Mapping of Ionospheric Electrodynamics (AMIE)
- Interactions of ionospheric fields with magnetospheric plasma
- Joule heating impacts on the thermosphere
- Low-latitude evening electrodynamics

Ionospheric Dynamo Modeling



S.V. Venkateswaran



S. Matsushita



Ray Roble



Cicely Ridley

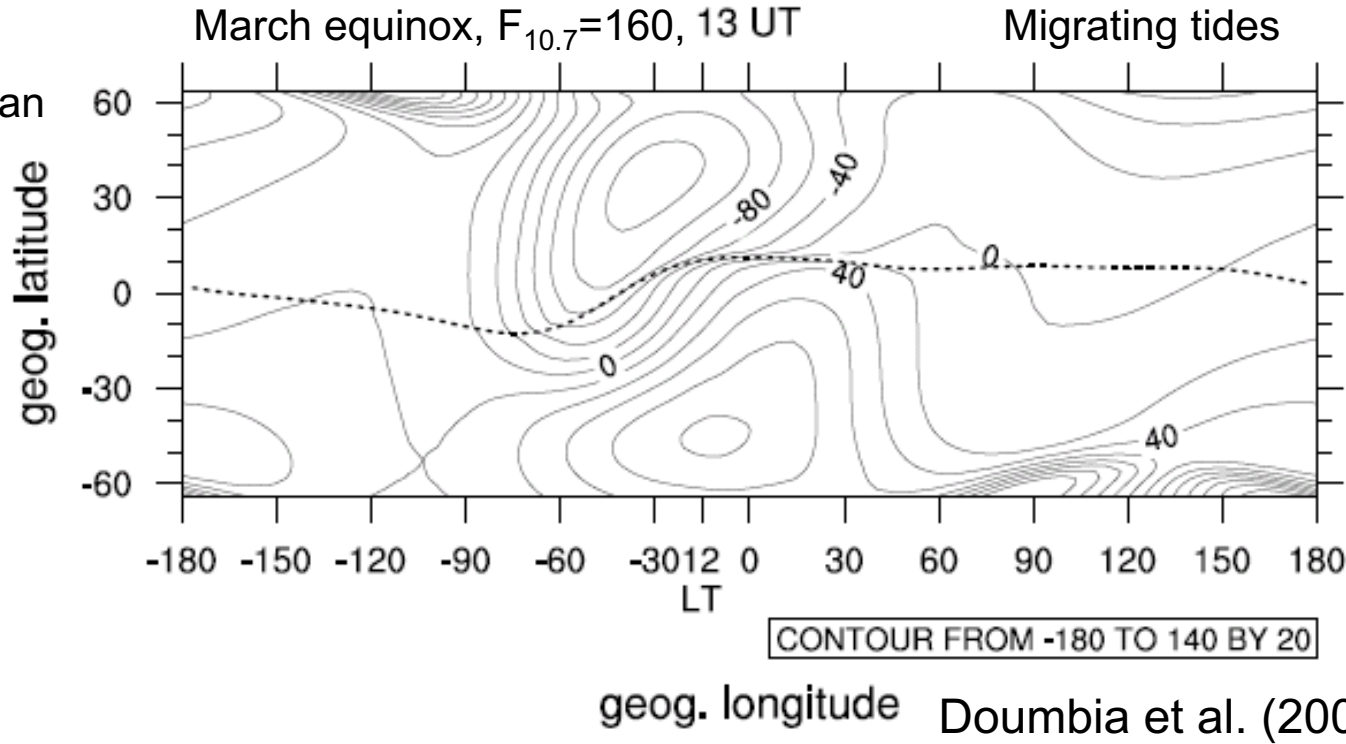


Cassandra Fesen



Tzu-Wei Fang

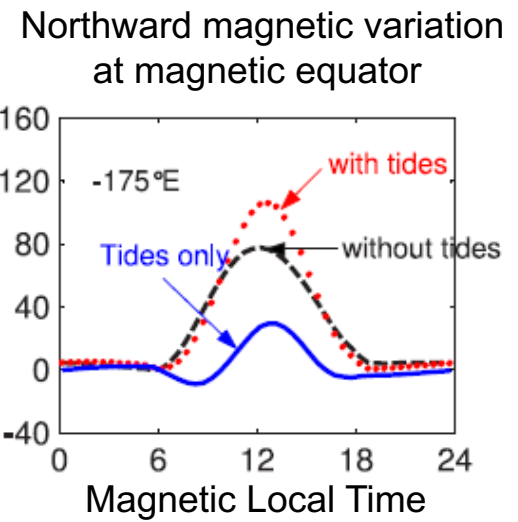
Equivalent Current Function, kA



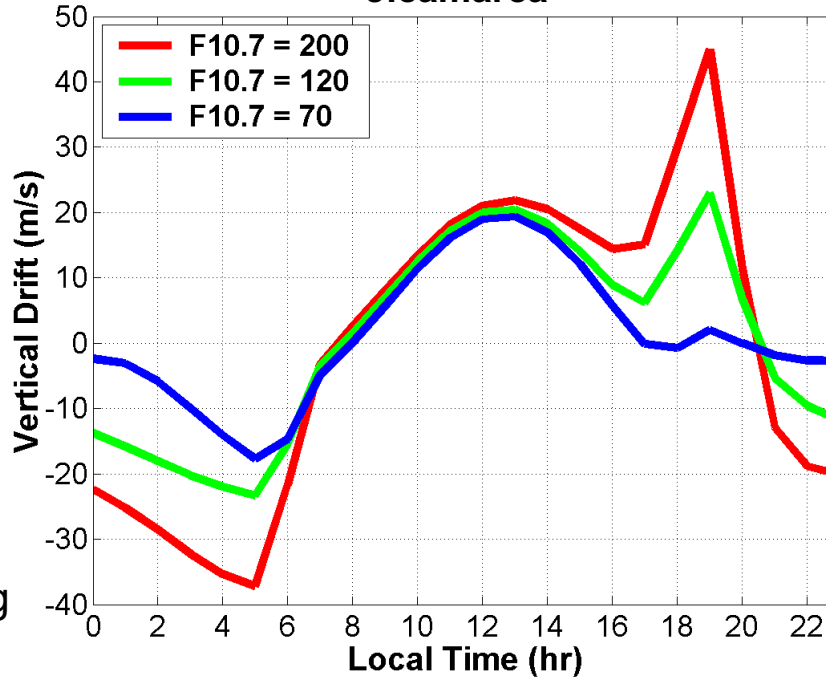
Vafi Doubia



Astrid Maute



Jicamarca



Ingrid Crossen



Patrick Alken

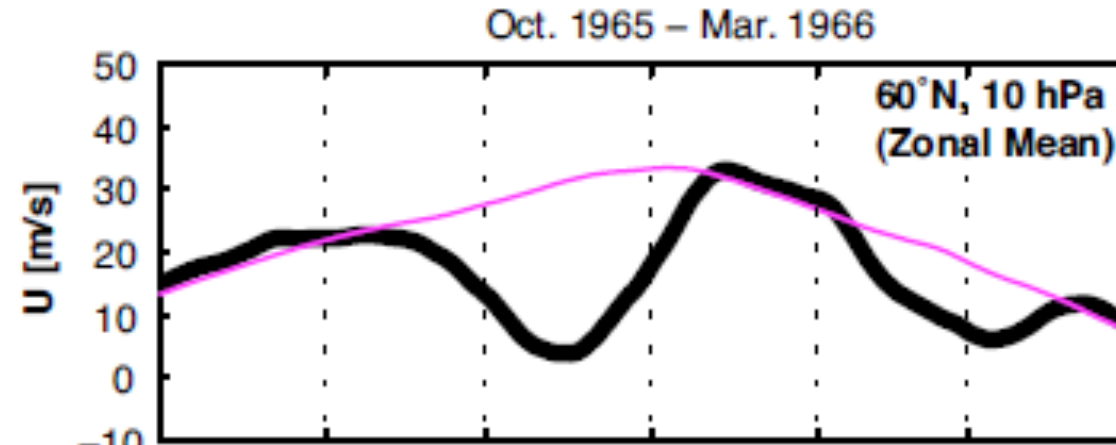
Lunar tidal response to stratospheric sudden warmings

Yamazaki et al. (2012)

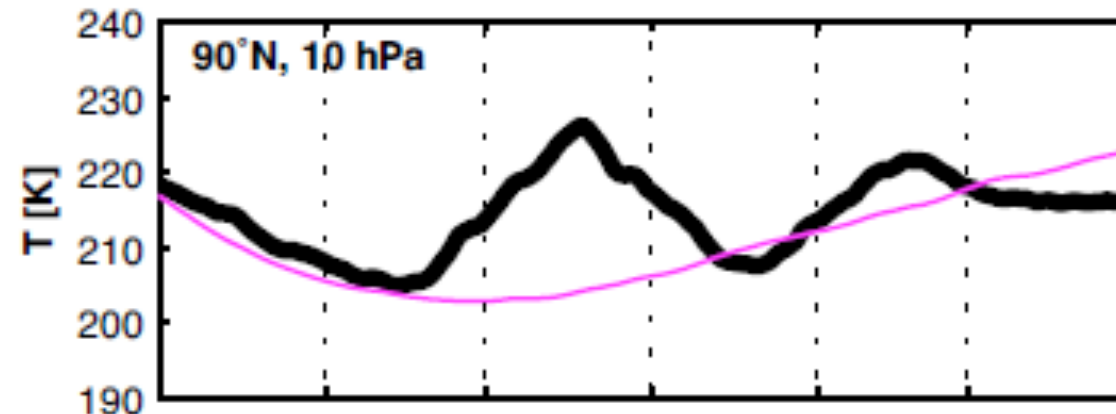


Yosuke Yamazaki

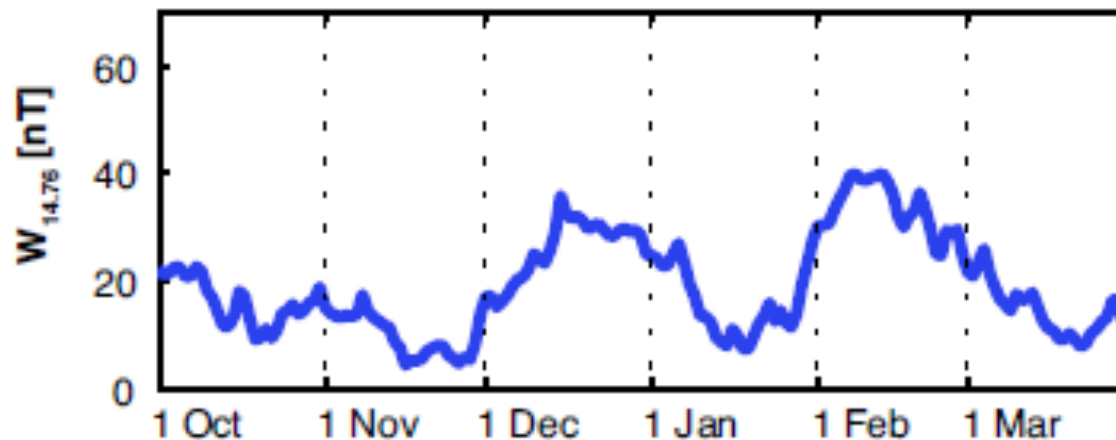
Stratospheric zonal-mean zonal wind at 60° N



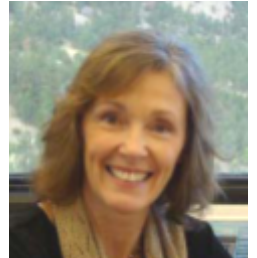
Stratospheric temperature at North Pole



Amplitude of 14.76-day geomagnetic perturbation at Addis Ababa



Robert Stening



Maura Hagan



Jeff Forbes



Nick Pedatella



Hanli Liu

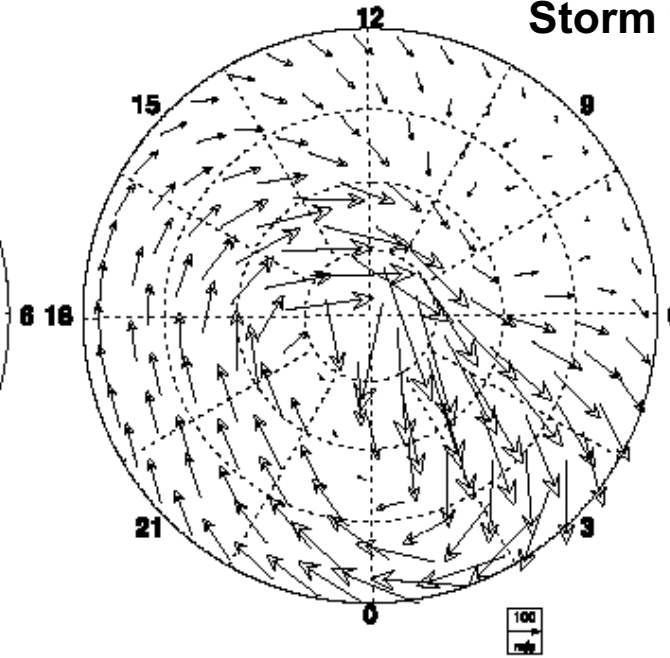
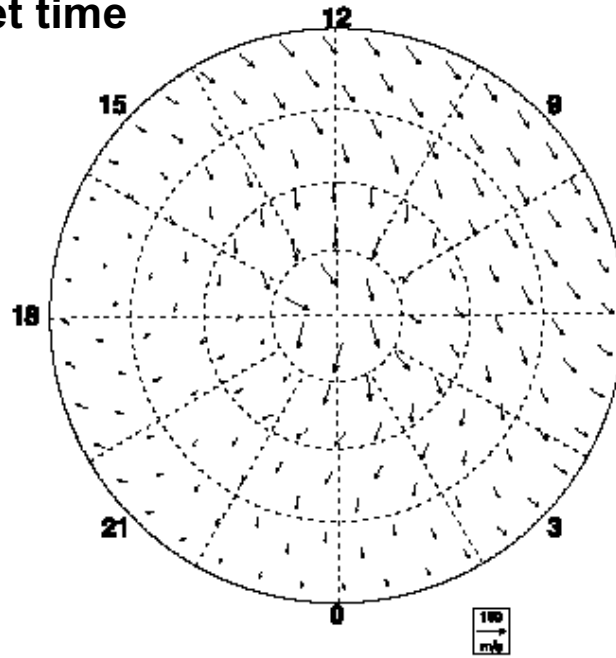
Wind, geomagnetic coordinates, 30-90 lat.

20 kV, 150 km

150 kV, 150 km

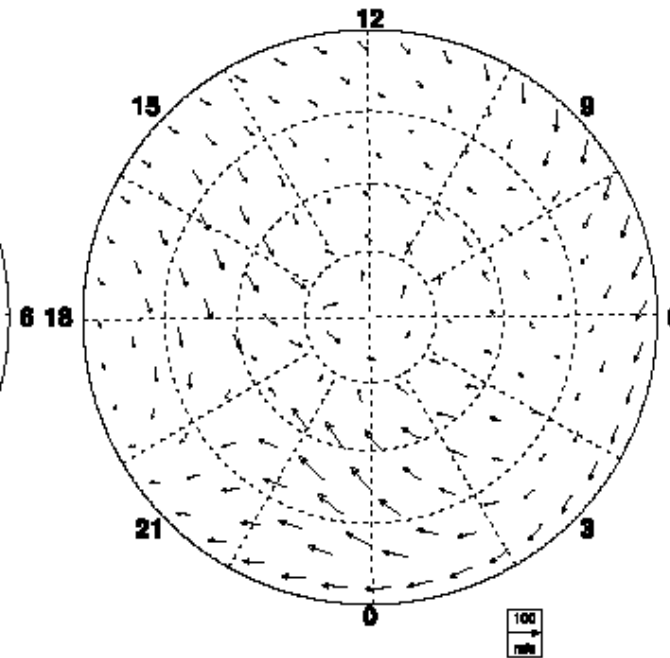
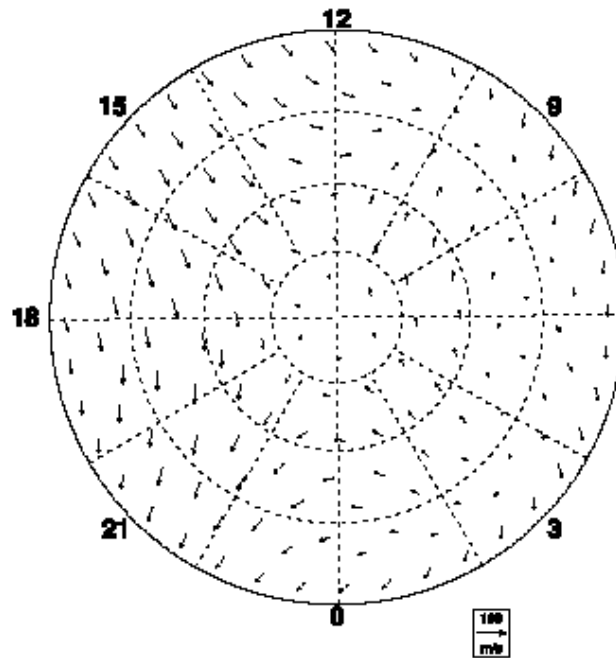
Quiet time

Storm time



20 kV, 110 km

150 kV, 110 km

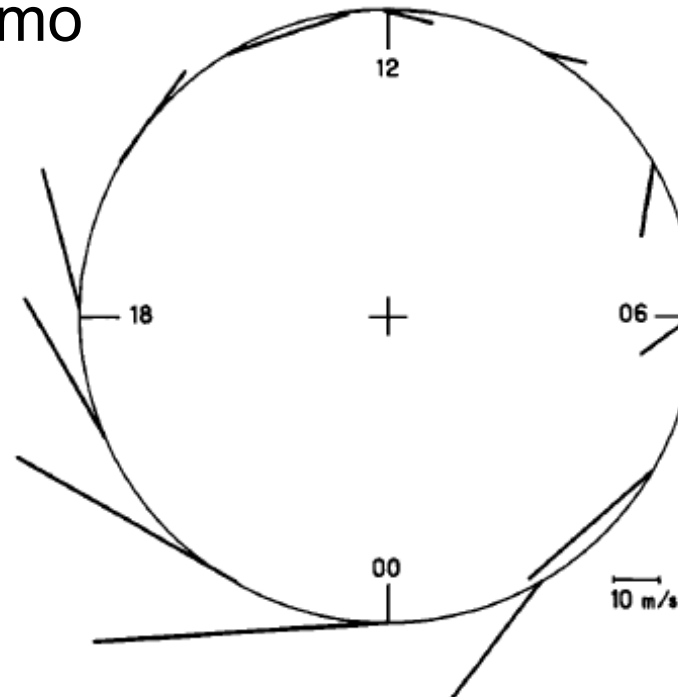


Ionospheric Disturbance Dynamo



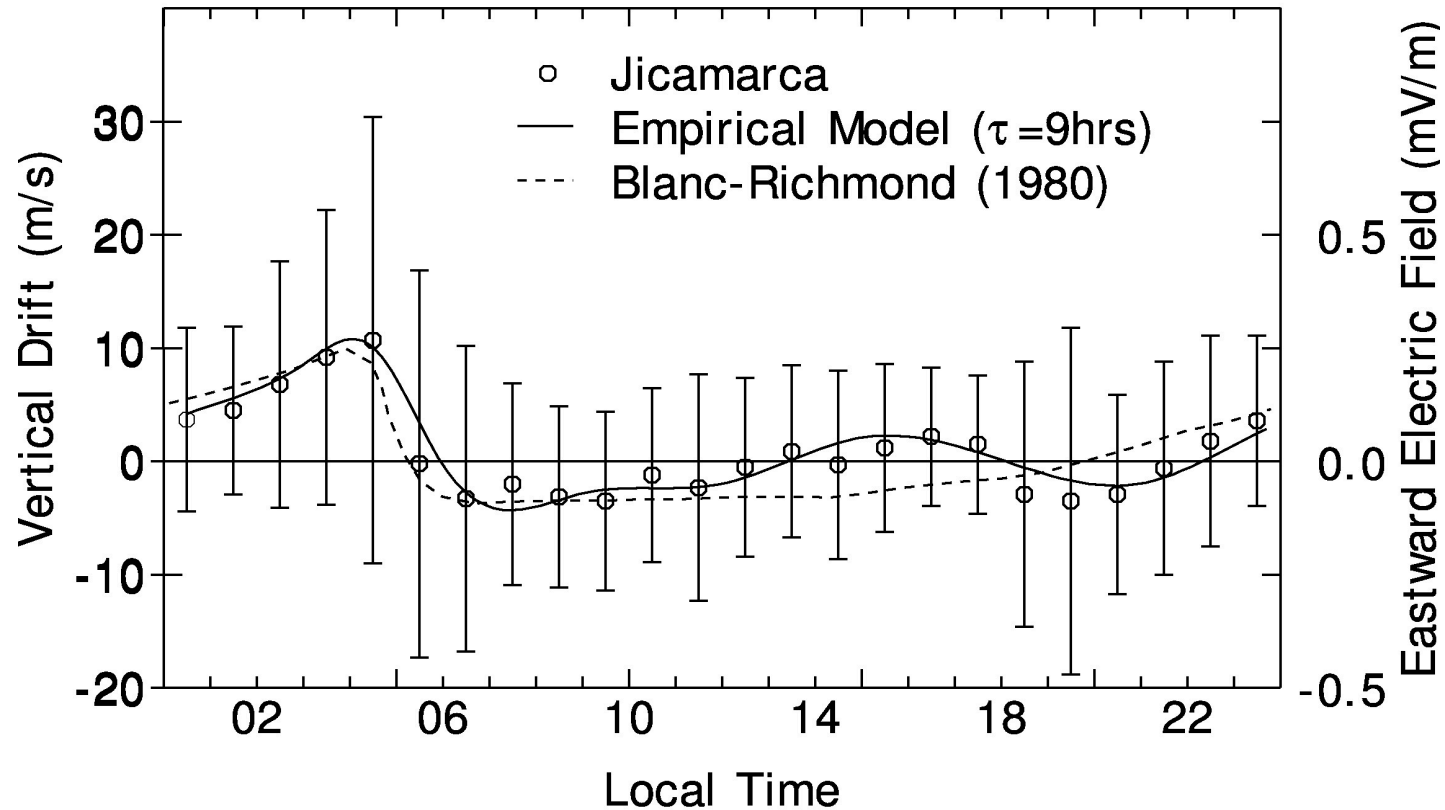
Michel Blanc

Average disturbed ($K_p > 2+$) minus quiet ($K_p \leq 2+$) drifts at Saint Santin (Blanc, 1978)

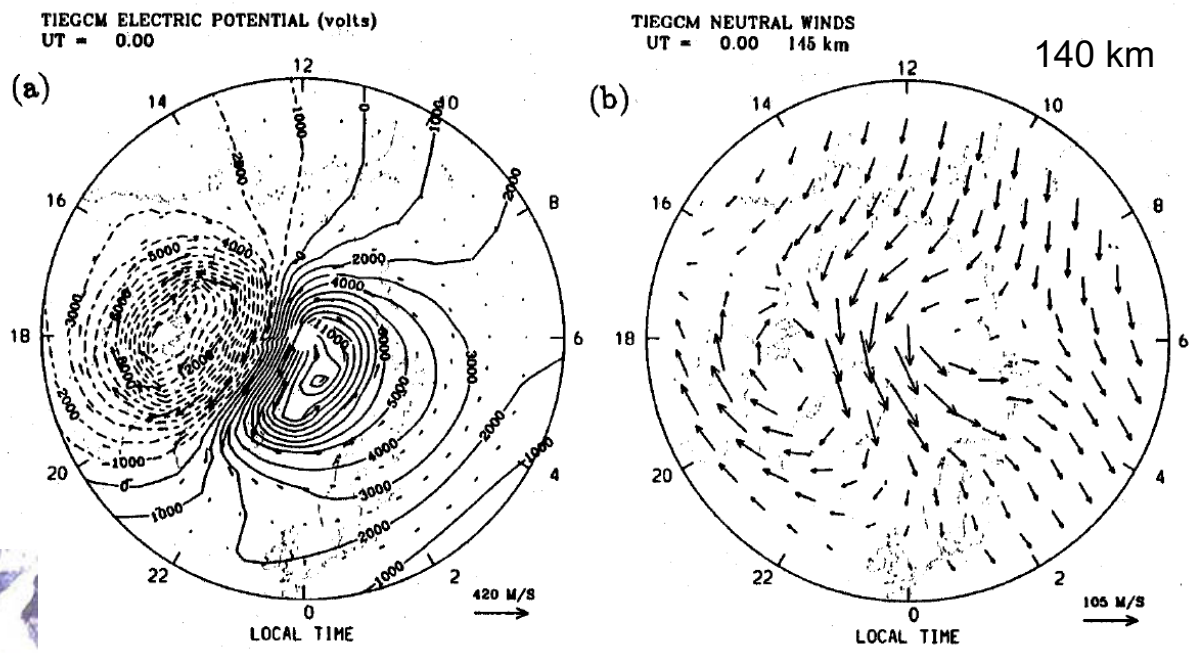


Christine Amory-Mazaudier

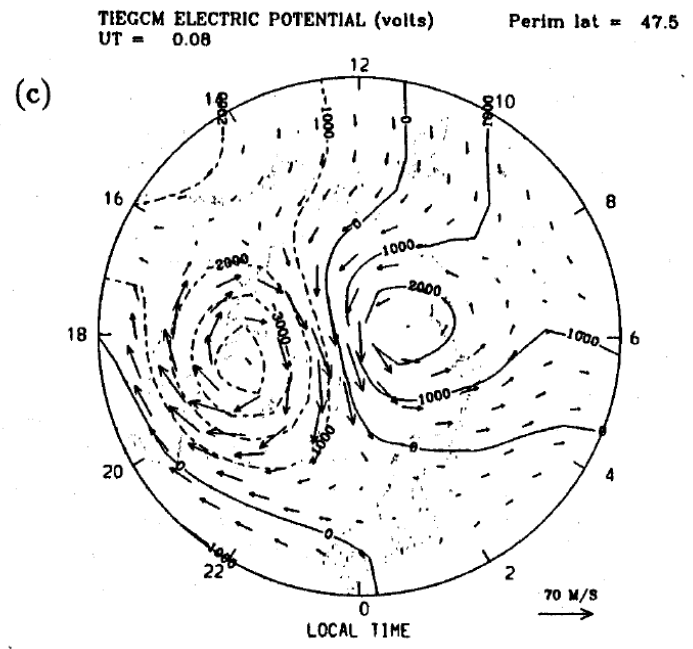
Scherliess and Fejer (1997)



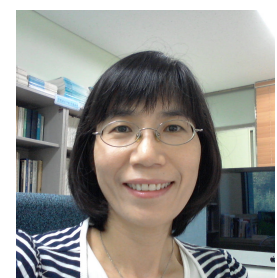
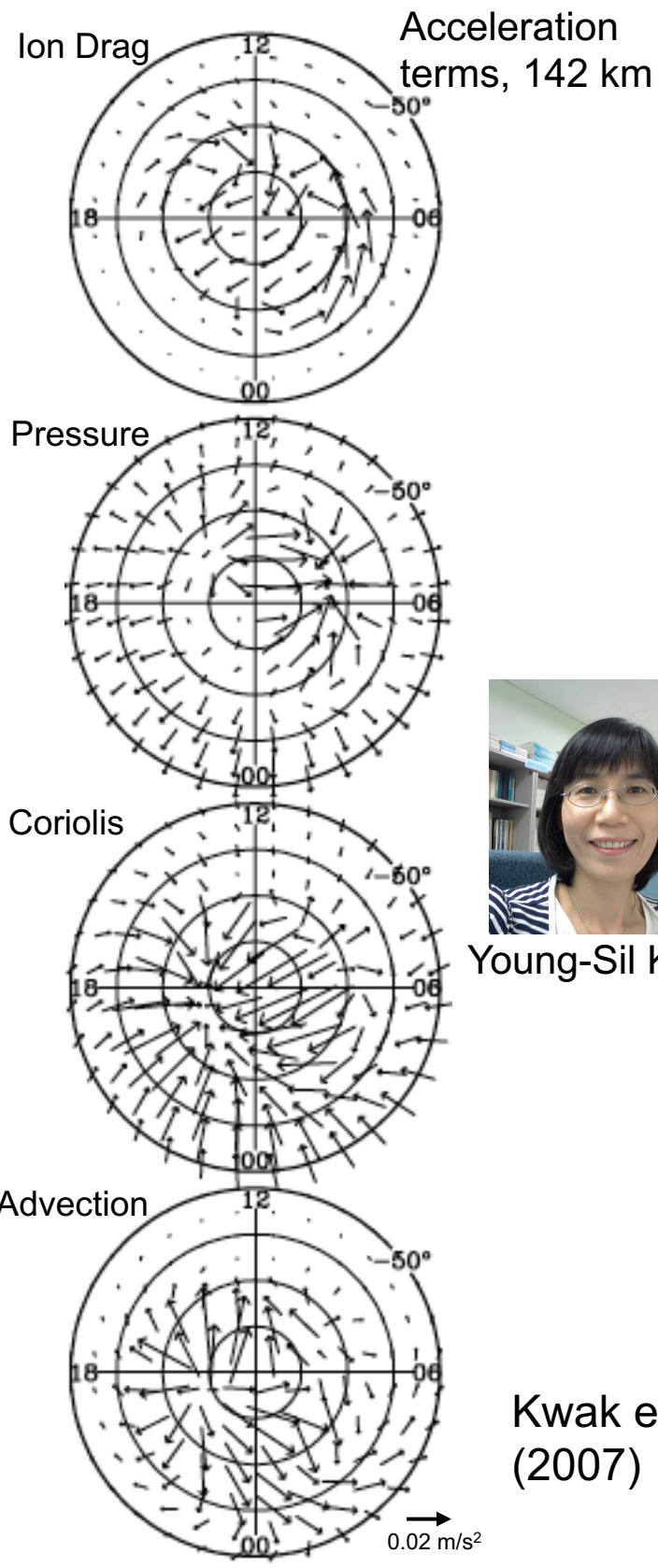
High-latitude Winds and "Flywheel" Effect



Ray Roble



Richmond (1995)



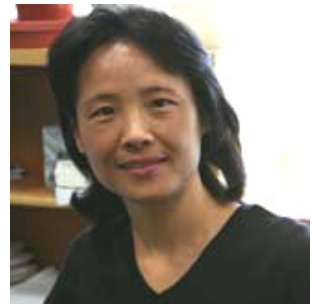
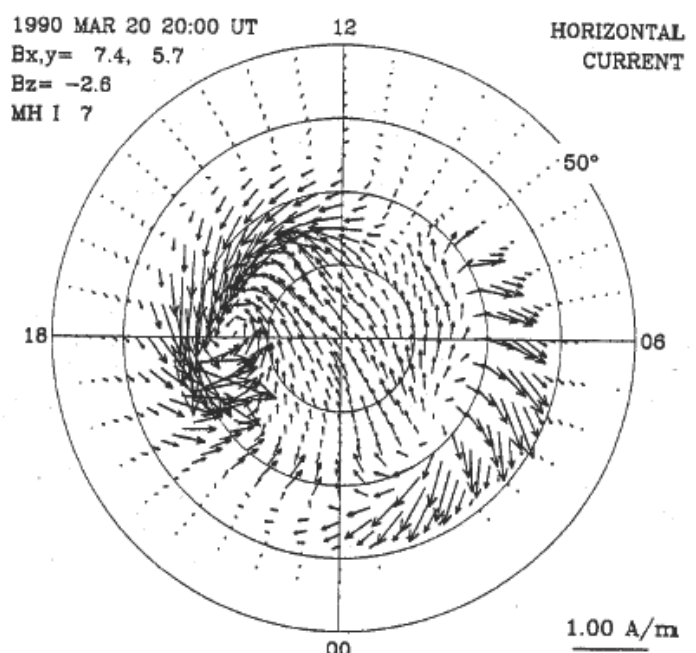
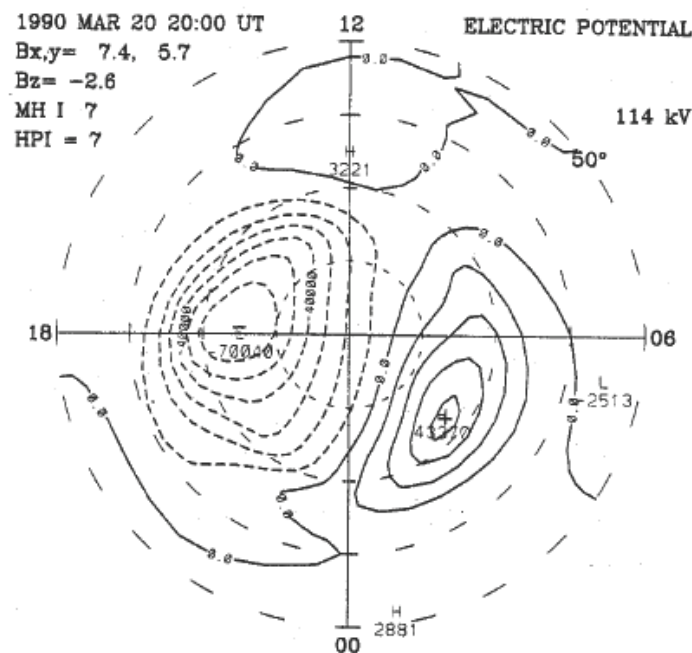
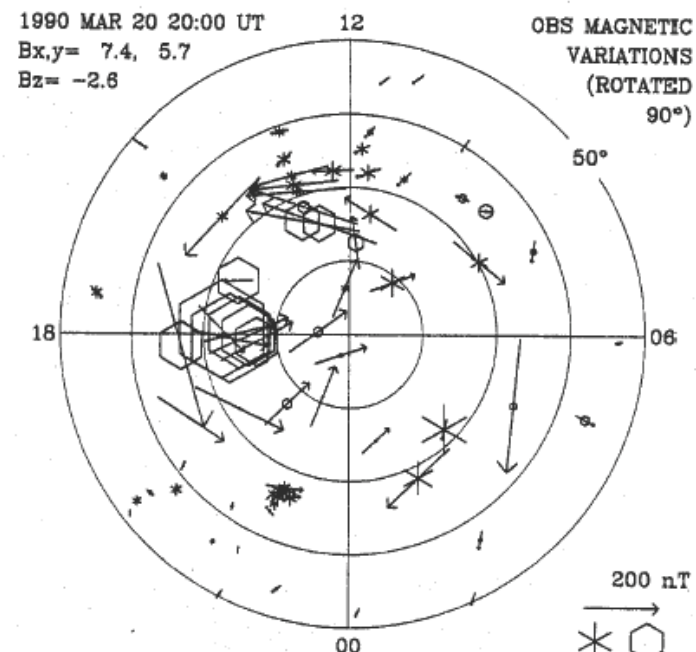
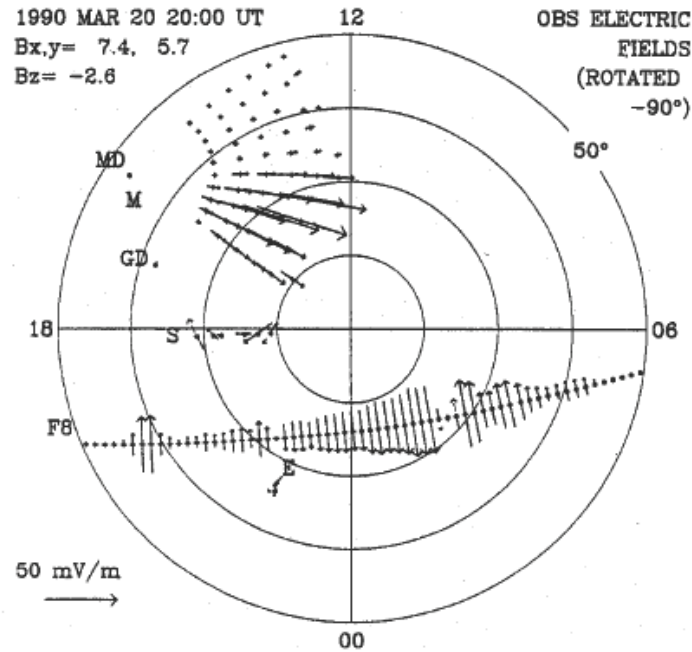
Young-Sil Kwak

Kwak et al. (2007)

ASSIMILATIVE MAPPING OF IONOSPHERIC ELECTRODYNAMICS (AMIE)



Yosuke Kamide



Gang Lu



Geoff Crowley



Aaron Ridley



Abena Poku-Awuah



Delores Knipp



Barbara Emery



Byung-Ho Ahn

SuperDARN Assimilative Mapping (SAM) procedure

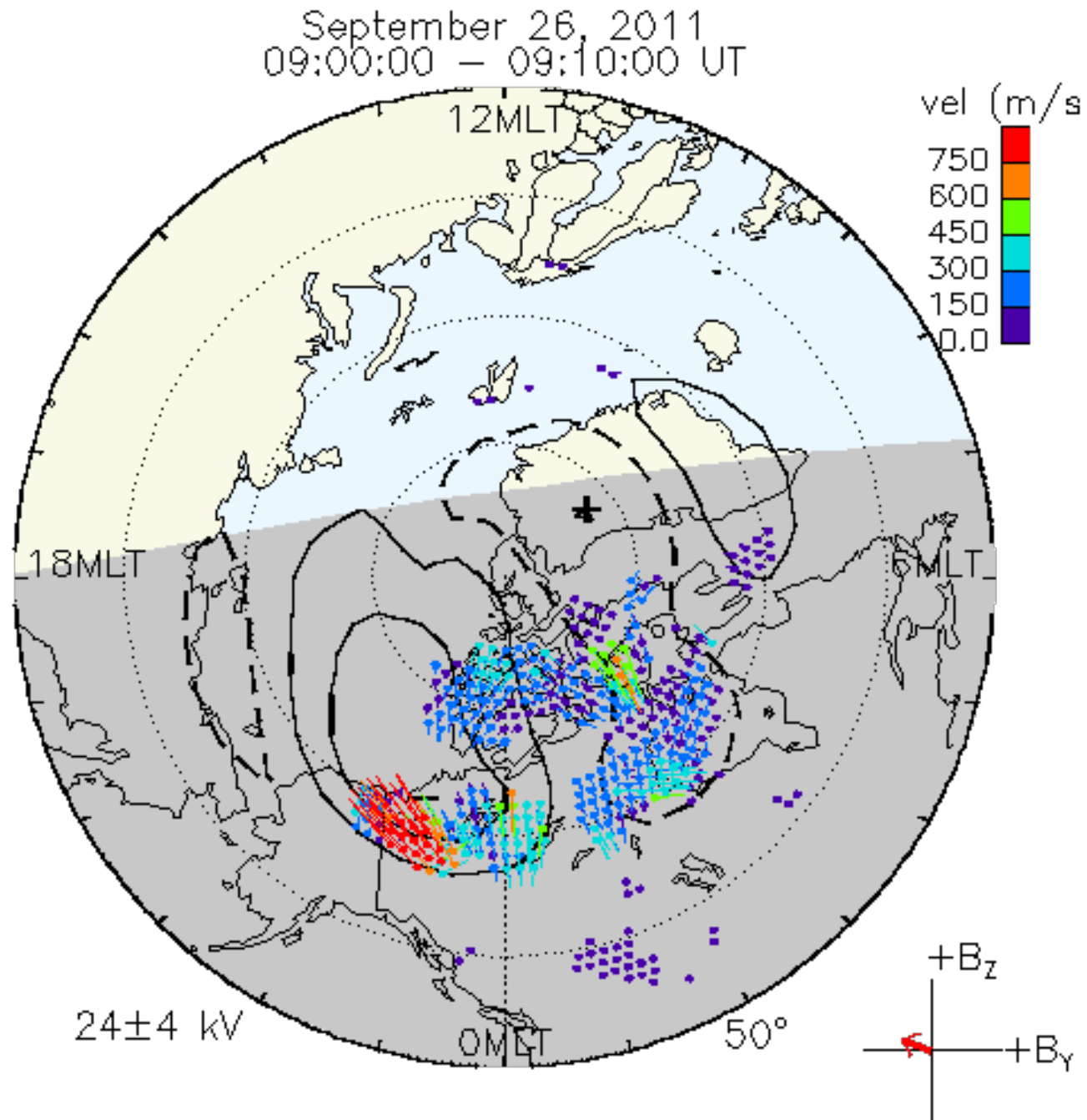
Cousins et al. (2013a,b)



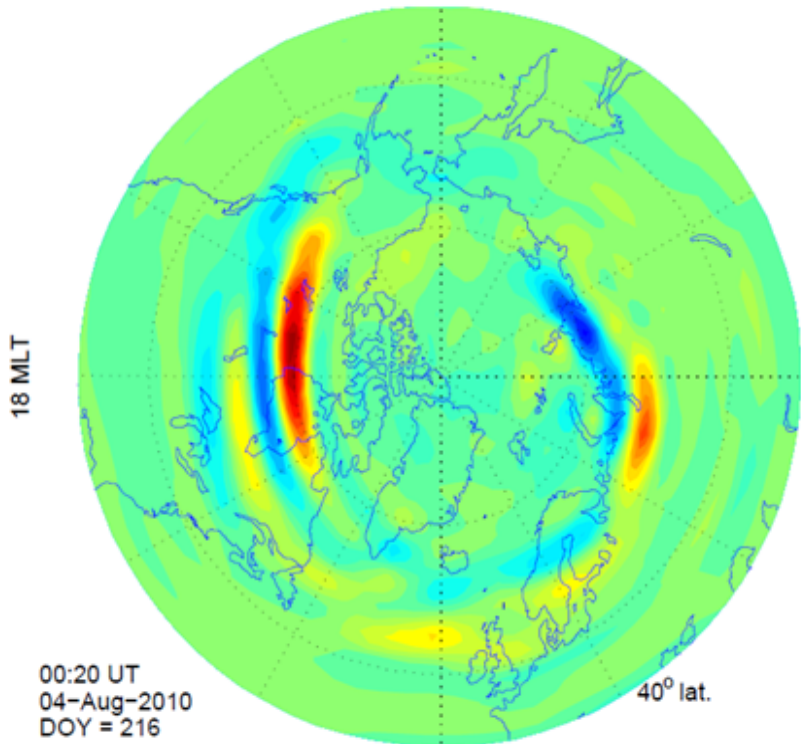
Ellen Cousins



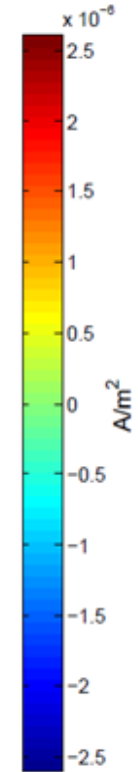
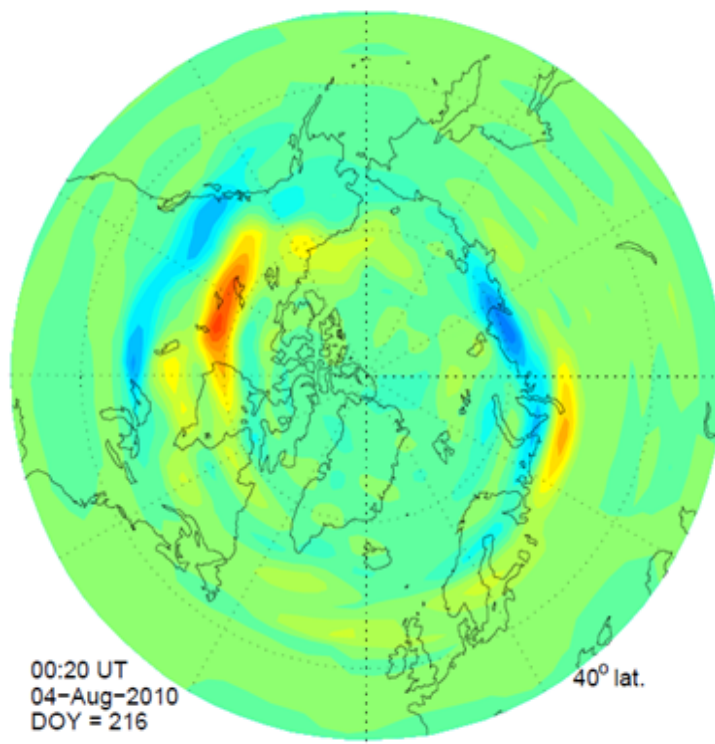
Tomoko Matsuo



AMPERE data
 J_r component of FACs (positive upward) - NH projection



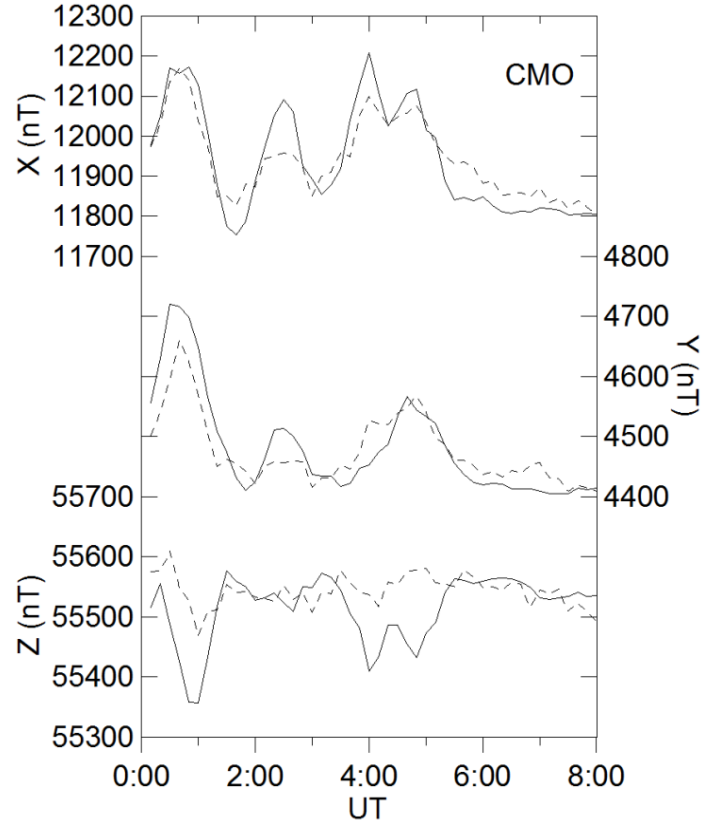
TIEGCM output - J_r (A/m²) - NH projection



AMPERE FAC in the TIEGCM can generate observed ground magnetic perturbations

Marsal et al. (2012)

00 MLT



— Observed
- - - Simulated



Santi Marsal



Brian Anderson

“Magnetic Mirroring” of Neutral Atoms

Galand and Richmond (1999)



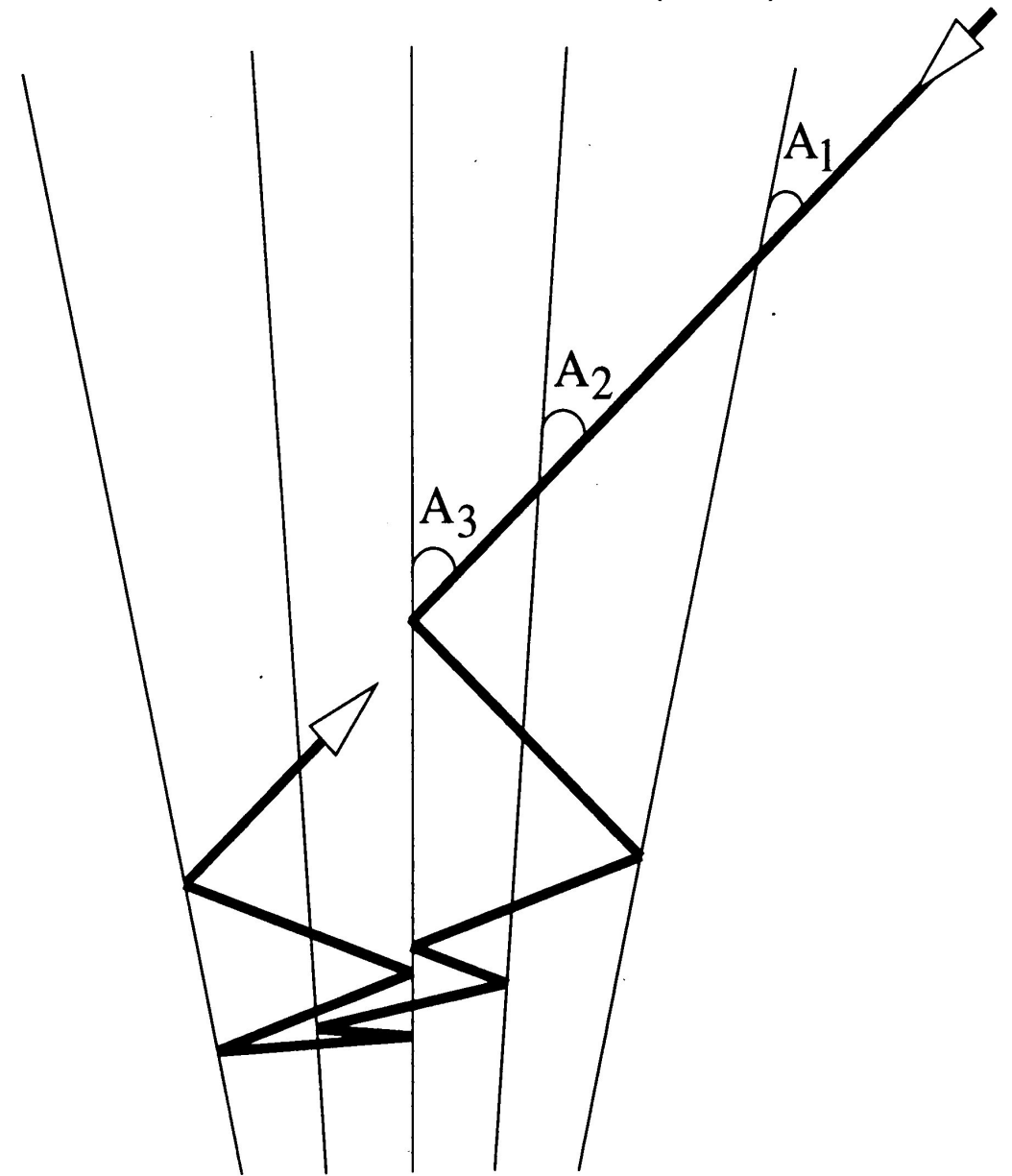
Marina Galand

Low-Latitude Ionization by Energetic Neutral Atoms

Lyons and Richmond (1978)



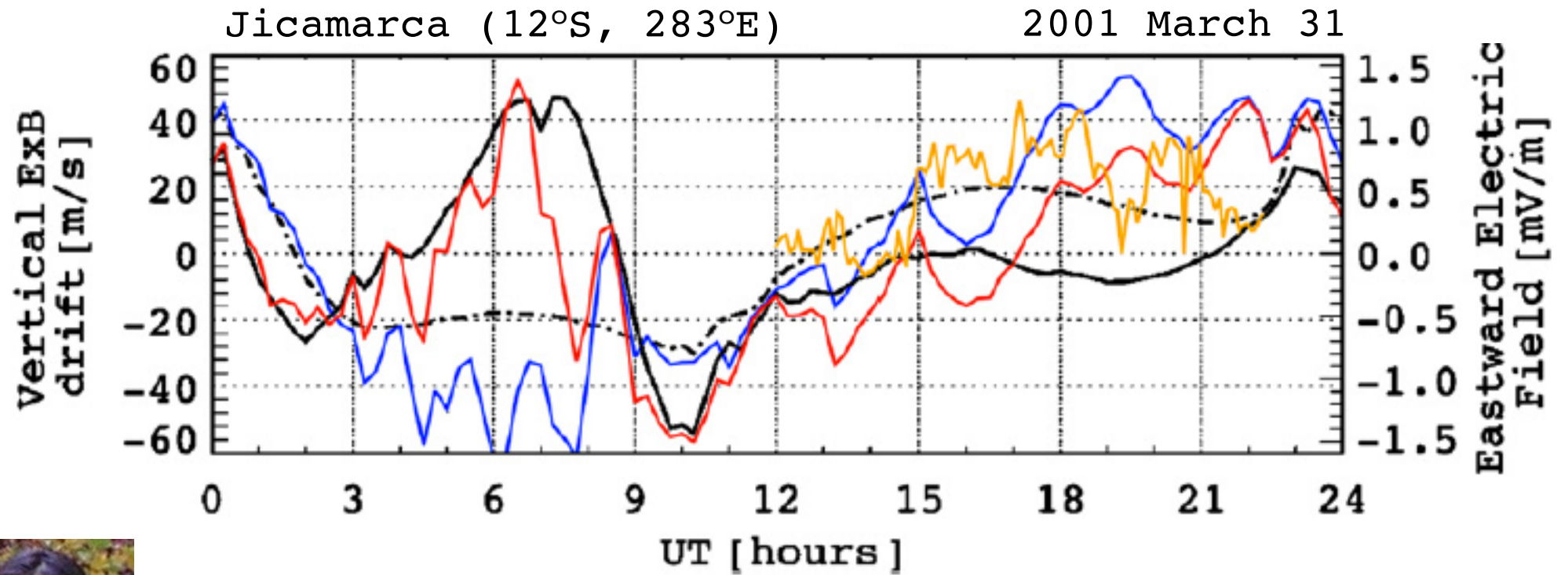
Larry Lyons



Storm-Time Electrodynamics:

Interactive Magnetosphere/Ionosphere/Thermosphere Modeling

Maruyama et al. (2007)



Naomi Maruyama



Tim Fuller-Rowell



Stan Sazykin

CTIPe/RCM simulations

Observation

- Quiet-time reference
- Wind only
- Hilat potential only
- Wind + Hilat potential
- Observation



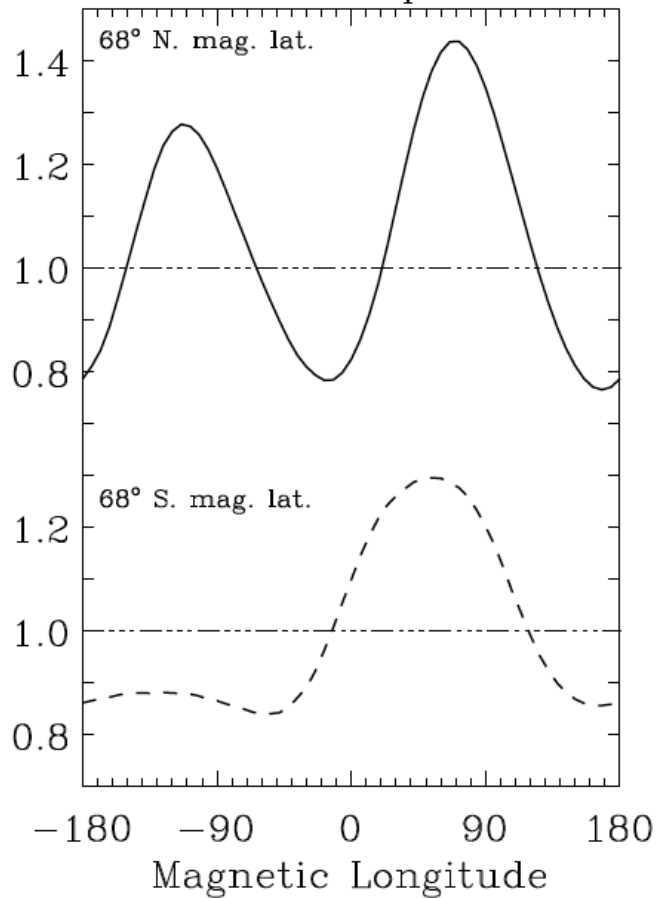
Christophe Peymirat



Arsene Koba

Non-Dipolar Geomagnetic Field Effects on Ionospheric Electrodynamics Calculated Using Magnetic Apex Coordinates

Joule Heating Per Unit
Magnetic Latitude/Longitude,
Normalized to Dipole Values



Gasda and Richmond (1998)

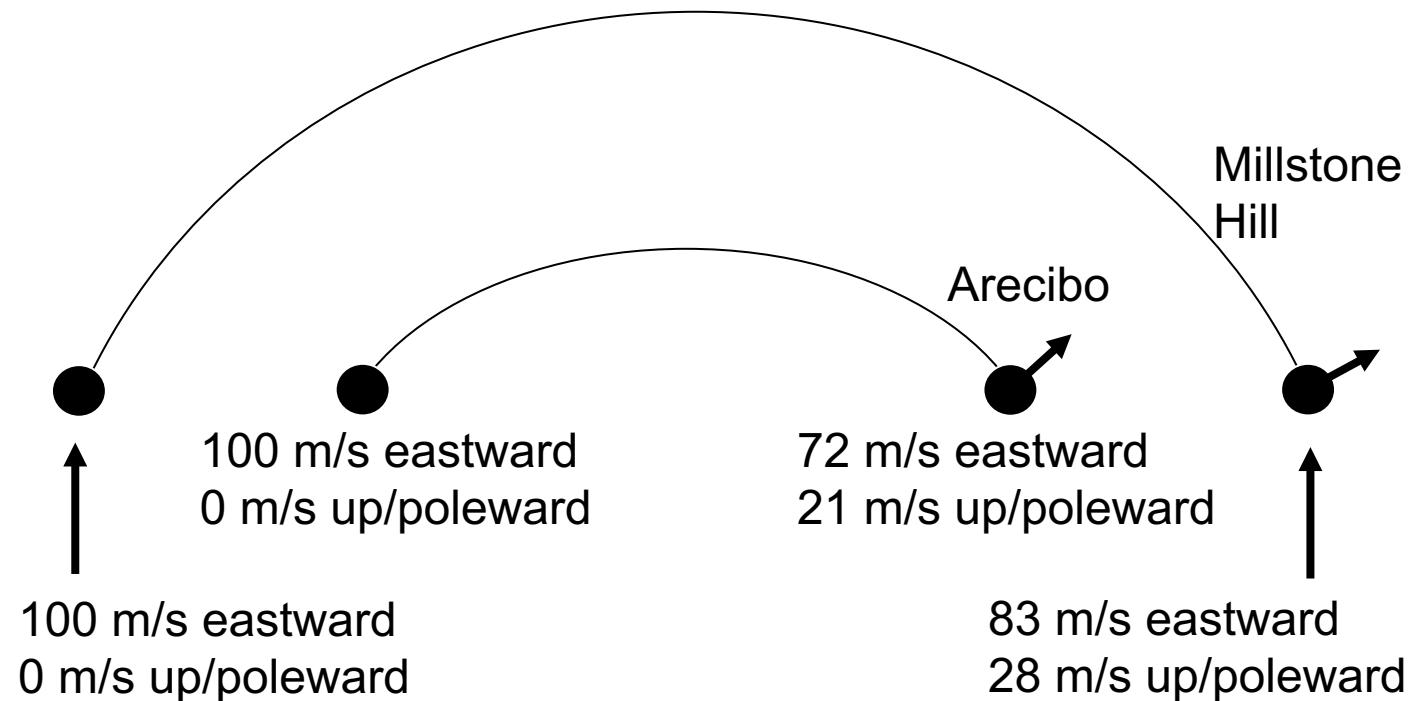


Sarah Gasda



John Emmert

Differences of \mathbf{ExB}/B^2 Velocities at Conjugate Points



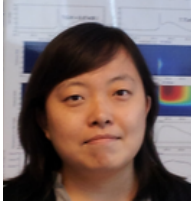
Emmert et al. (2010)
Laundal and Richmond (2017)



Karl Laundal

Density Response at 400 km to Joule Heating at Different Heights

Huang et al. (2012)

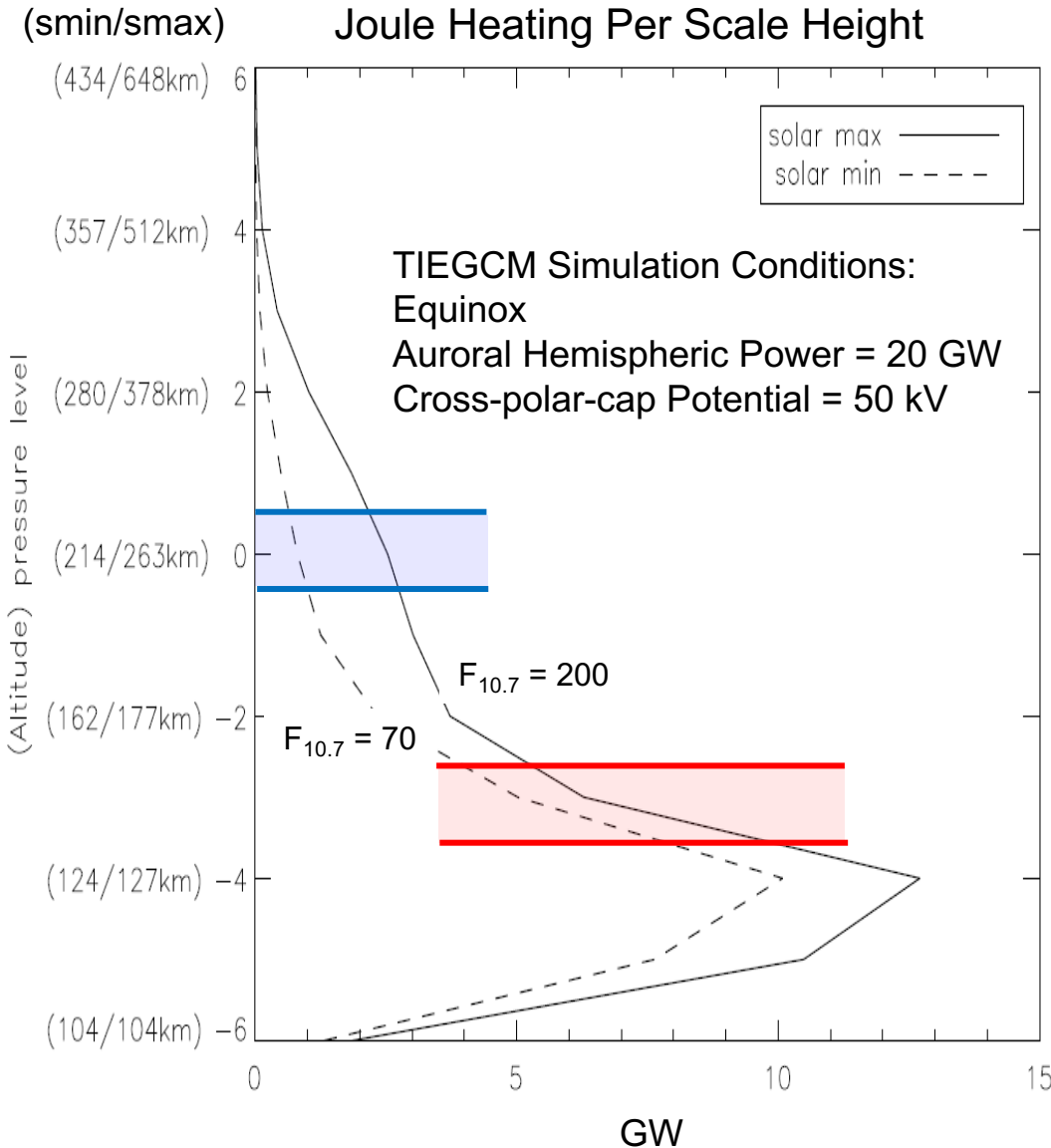


Yanshi Huang

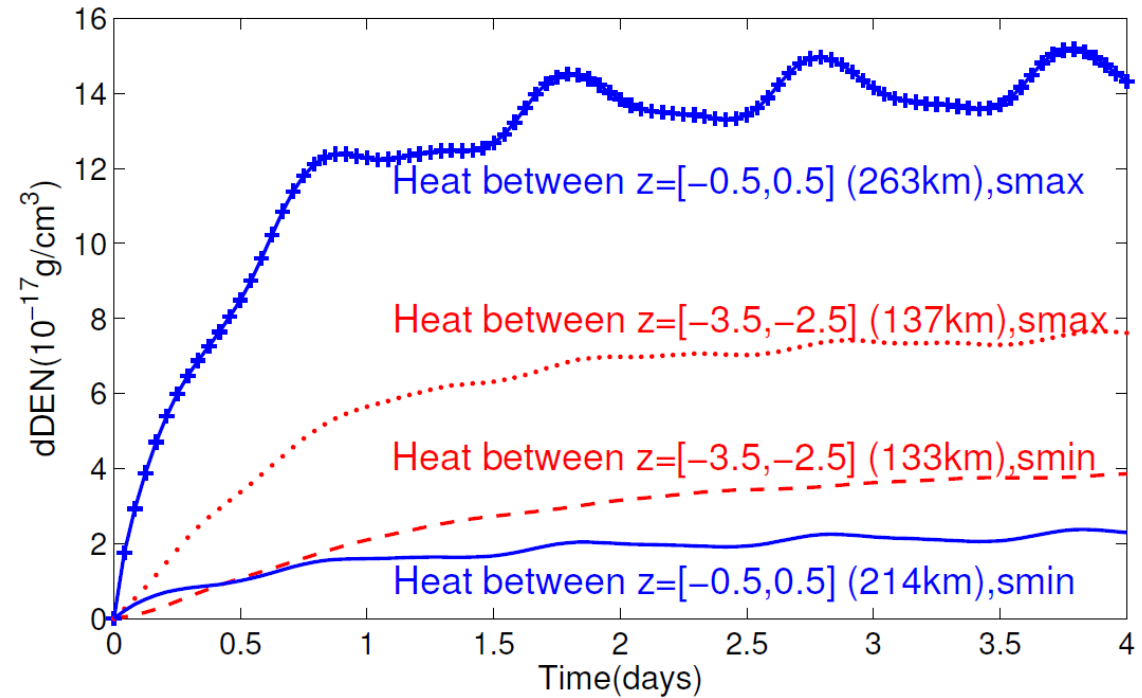


Yue Deng

Globally Integrated
Joule Heating Per Scale Height



Contributions to Density Perturbations at 400 km

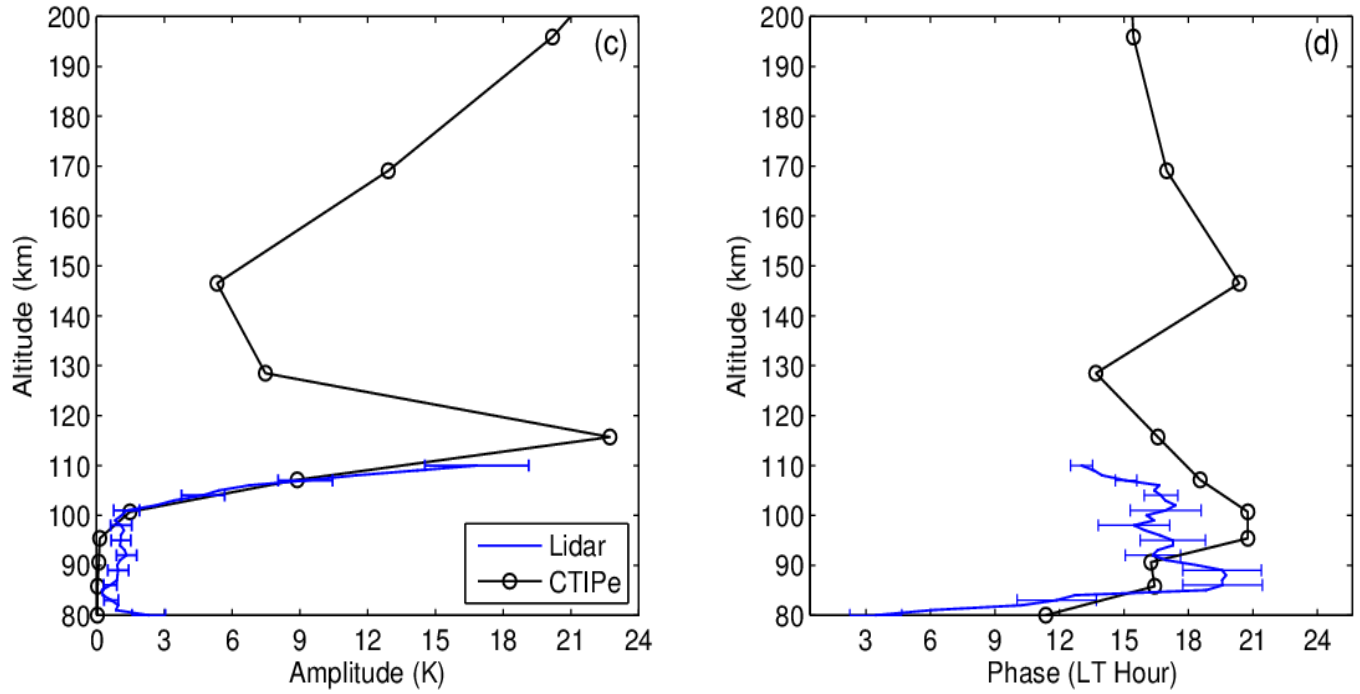


Much more Joule heat is deposited in the **E region** than in the **F region**, but **F-region** heating dominates the density response during at least the first 12 hours of a storm, especially at solar maximum.

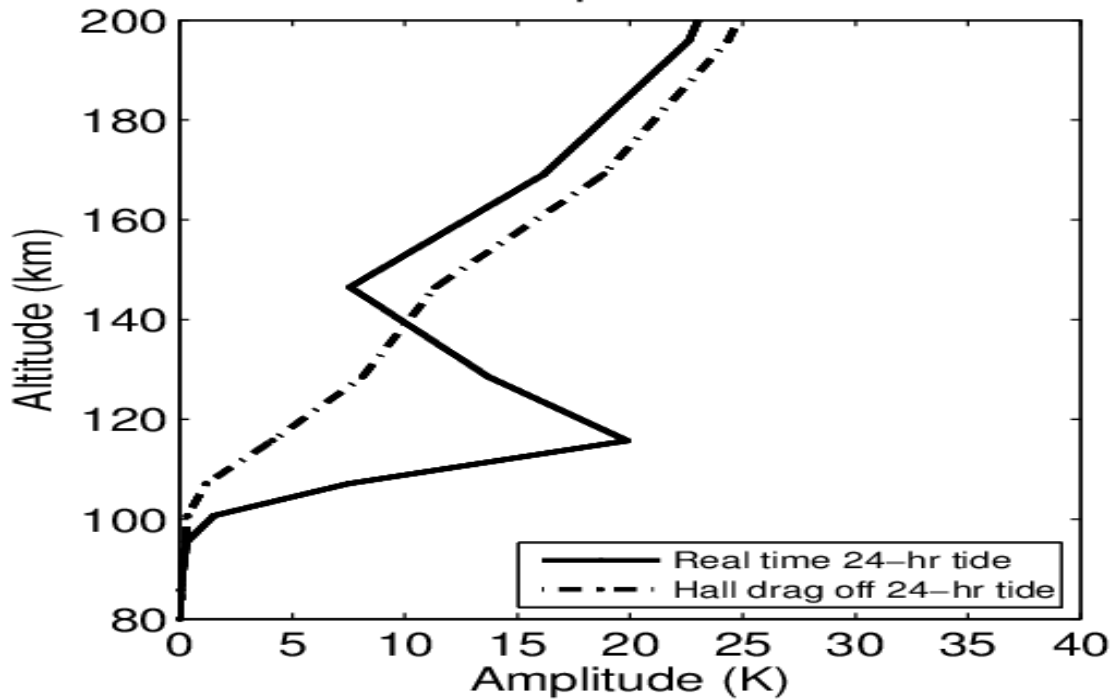
Rapid Altitude Growth of Diurnal Tide in Temperature at McMurdo

Fong et al. (2015)

Four Years Lidar Diurnal Tide



Diurnal Amplitude at McMurdo



Weichun Fong



Xinzhao Chu

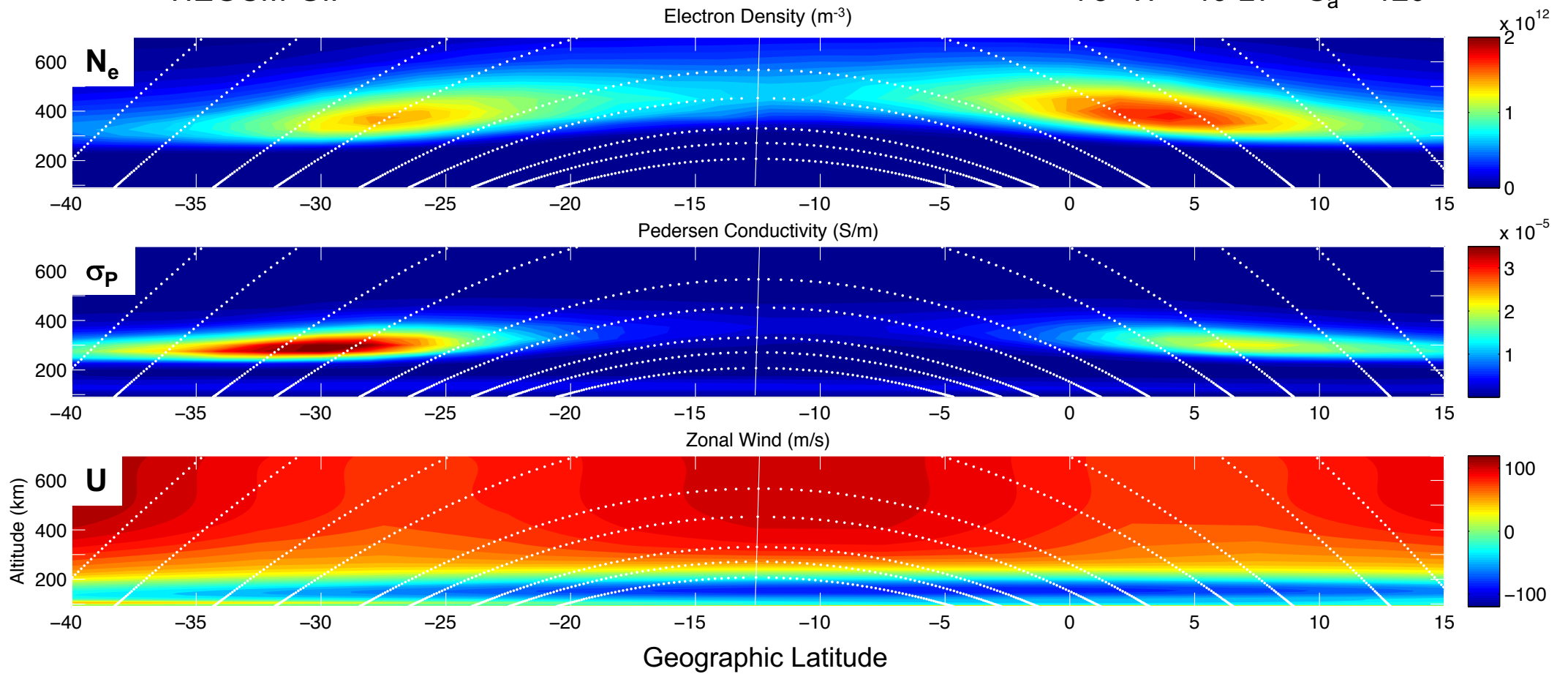


Tim Fuller-Rowell

Low-Latitude Evening Electrodynamics

TIEGCM-GIP

75° W 19 LT $S_a = 120$



Tzu-Wei Fang



Astrid Maute

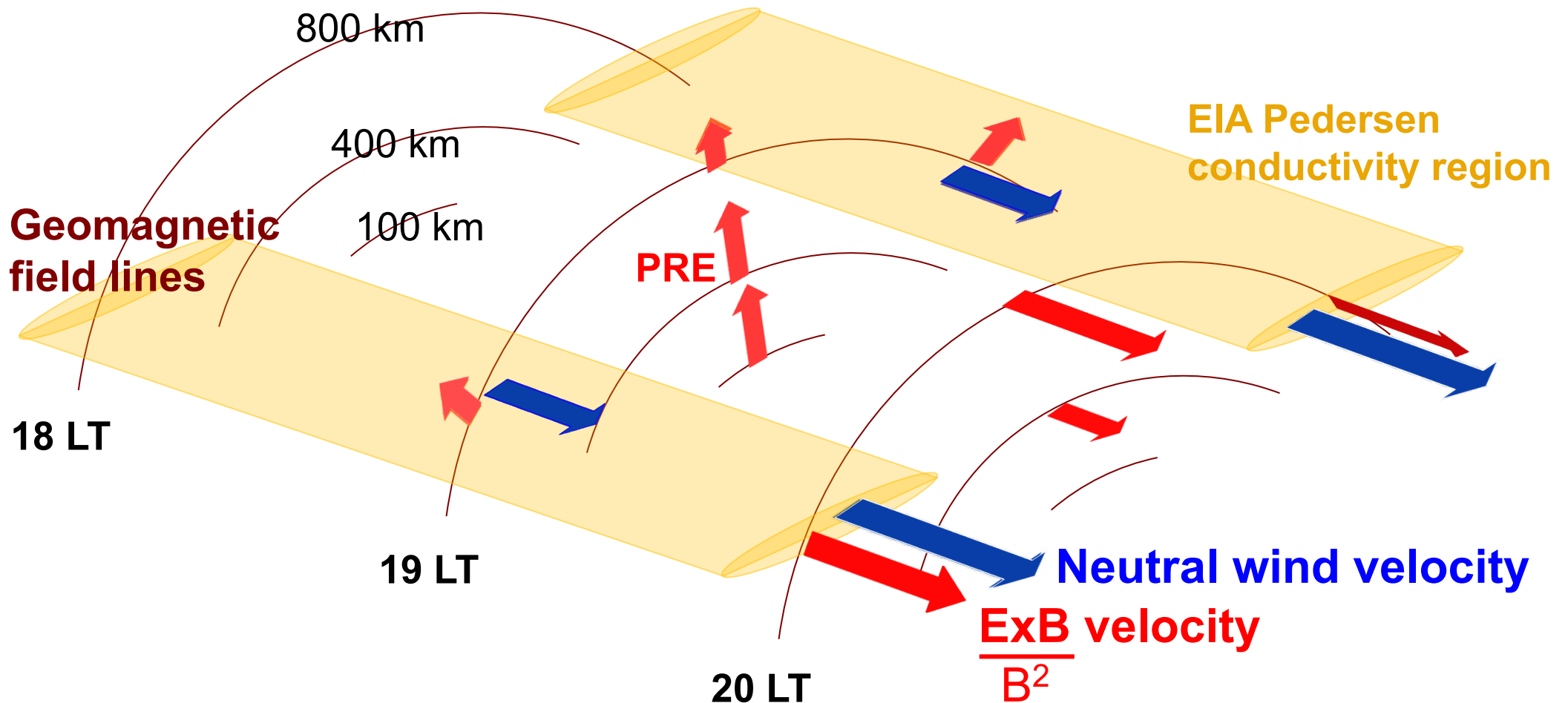


Will Evonosky

Richmond et al. (2015)

Richmond and Fang (2015)

Evonosky et al. (2016)



- ExB convection is practically constant along magnetic field lines.
- Differences between neutral wind velocity and ExB velocity create drag on convection.
- Eastward neutral wind at EIA latitudes increases with height and toward the east, tending to drag plasma along.
- Continuity of ExB convection requires vertical inflow around 18.5-19 LT, producing pre-reversal enhancement (PRE) of vertical drift around 400 km.
- Upward ExB convection extends through E region, where the equatorial electrojet exerts drag on the convection.

Concluding Remarks

Ionospheric electrodynamics involves interactions:

- ionization processes
- ionosphere dynamics
- neutral dynamics
- tides and waves (coupling with lower atmosphere)
- coupling with magnetosphere

It therefore requires collaborative research.

Advancements call for:

- extensive observations
- whole-atmosphere modeling
- coupled magnetosphere/ionosphere/atmosphere modeling
- data assimilation